

D-D neutron yield in the 125 J dense plasma focus Nanofocus

M. Milanese, R. Moroso, and J. Pouzo^a

Instituto de Física Arroyo Seco, Universidad Nacional del Centro de la Provincia de Buenos Aires and CONICET, Tandil, Argentina

Received 25 February 2003 / Received in final form 29 April 2003

Published online 5 August 2003 – © EDP Sciences, Società Italiana di Fisica, Springer-Verlag 2003

Abstract. We present here a very small transportable dense plasma focus with 125 J of energy able to be used mainly as an intense fast neutron source. The aim of this work was to design, construct and experimentally study a very compact nuclear fusion apparatus, at the lower energy limit, useful for multiple applications, such as soil humidity measurements, inspection of several materials metallic inclusions, medical neutron-therapies, etc. Besides, the possibility of using the same device as X-rays emitter has been explored. In a narrow range of deuterium filling pressure around 1 mbar, peaked Rogowski dips are observed. Correspondingly, strong neutron and hard X-ray pulses are measured. The neutron pulses last, in average, 50 ns, being about 10^6 the amount of neutrons per pulse. The performance of this device has shown to be higher than any other plasma focus apparatus, compared on the empirical scaling law of neutron yield *vs.* pinch current.

PACS. 52.58.Lq Z-pinches, plasma focus and other pinch devices – 52.70.Ds Electric and magnetic measurements – 52.70.Nc Particle measurements

1 Introduction

The plasma focus is a compact pulsed plasma generator, which is able to give intense neutron pulses, soft and hard X-rays bursts and ion and electron beams [1–5]. It consists, basically, in a pair of coaxial electrodes immersed in gas at low pressure. The driver of the device is based in a fast capacitor bank. A plasma sheath is formed on the coaxial insulator that separates both electrodes, then it moves along the anode, rolls off it, the plasma cylinder is compressed by pinch effect and, finally, a zone of hot (around 1 keV) and dense (around 10^{20} cm⁻³) plasma is formed. There fast electron and ion beams are produced; radiation is detected for a wide range of wavelengths (by instance soft and hard X-ray bursts). If pure deuterium or a mix of deuterium and tritium is used as filling gas, also pulses of neutrons and ions generated in nuclear fusion reactions are registered. A schematic of the coaxial and radial compression stages of the plasma sheath evolution is shown in Figure 1. The plasma focus experiments used for studies ranged, up to now, from some hundred joules to megajoules (see Refs. [6–14]). Besides the big or medium machines that contribute with important data to the development of plasma physics, many table-top plasma focus experiments (see PACO at Tandil [9] and other [4, 7, 14, 15]) show that basic plasma studies and also a lot of applications are suitable in low-energy scale. Although the basic plasma physics studies and as energy generator, some applications that can be mentioned are: soft

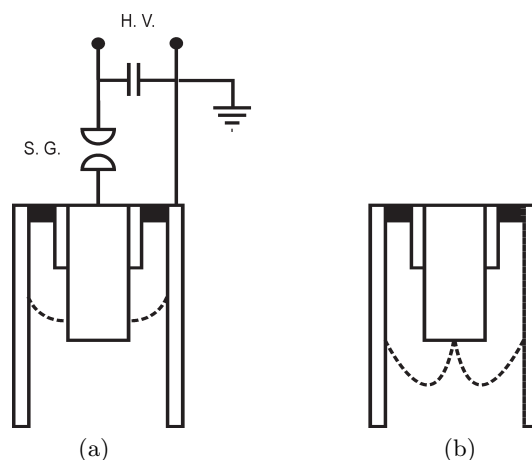


Fig. 1. Schematic of plasma sheet: (a) in the coaxial stage and (b) radial compression stage.

X-ray microscopy [16], X-ray backlighting and soft X-ray and electron beam lithography [17], radiographs of small and very mobile living specimens [18, 19], calibration of dark matter detectors [15]. Other potential uses are related with nuclear fusion reactions, *e.g.*, studies on reactors, neutron therapies, neutron-graph, neutron attenuation in soil. This last mentioned application has mainly motivated the present work. Because of the importance of the device compactness and efficiency, looking forward the above mentioned and other applications, we designed and constructed, in a work that began in 1999, a very little

^a e-mail: pouzo@exa.unicen.edu.ar

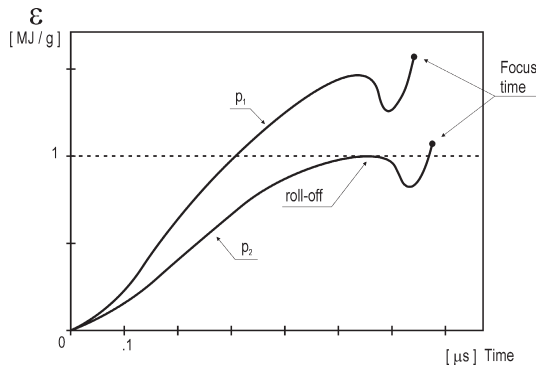


Fig. 2. Typical curves of the electromechanical work performed on a deuterium plasma focus sheath by mass unit ε as a function of time for two different values of the pressure p_1 and p_2 . The horizontal dotted line indicates the specific ionisation energy of deuterium.

size plasma focus compatible with high neutron production [20–22].

In this article the design, construction and results, including nuclear fusion neutrons detection, of the very compact and portable 125 J plasma focus Nanofocus is presented.

2 Design of the Nanofocus

This generator is designed taking into account technological and physical constraints. The Mather-type plasma focus (PF) concept is chosen. A computational code [23] is used to optimise the PF parameters respect to 2.45 MeV neutron yield, product of the deuterium–deuterium nuclear fusion. The starting point was obtain a device with minimal dimensions able to be used in the country, because of one of the objectives mentioned above: measurement of soil humidity for application in agronomy.

One of the design criteria is that the PF must fulfil the following condition: the electromechanical work by mass unit at the roll-off time should be higher than the specific ionisation energy of deuterium (see Fig. 2 and also Ref. [9]). This energy per unit mass must be high but not too much, because preheating shocks could be present inhibiting a good compression. The plasma focus experiments whose design fulfils the criteria stated in reference [24] are well aligned in the curve $Y = kI_p^{4.7}$ (see Fig. 3). In the last expression Y is the neutron yield in a discharge, I_p is the pinch current and k is a constant (k approx. 2×10^8 when I_p is measured in MA). Such behaviour can be explained from a thermonuclear model being the plasma magnetically confined in the radial direction and inertially confined in the axial direction [24]. In Figure 3 it can be seen that the small plasma foci go out to the straight-line, that is, their efficiency regarding the neutron yield is higher. This characteristic indicates a possible major incidence in small devices of another nuclear interaction mechanism: beam-target, which is present together with the thermonuclear effect in every PF discharge. The model used here has well-predicted experimental results

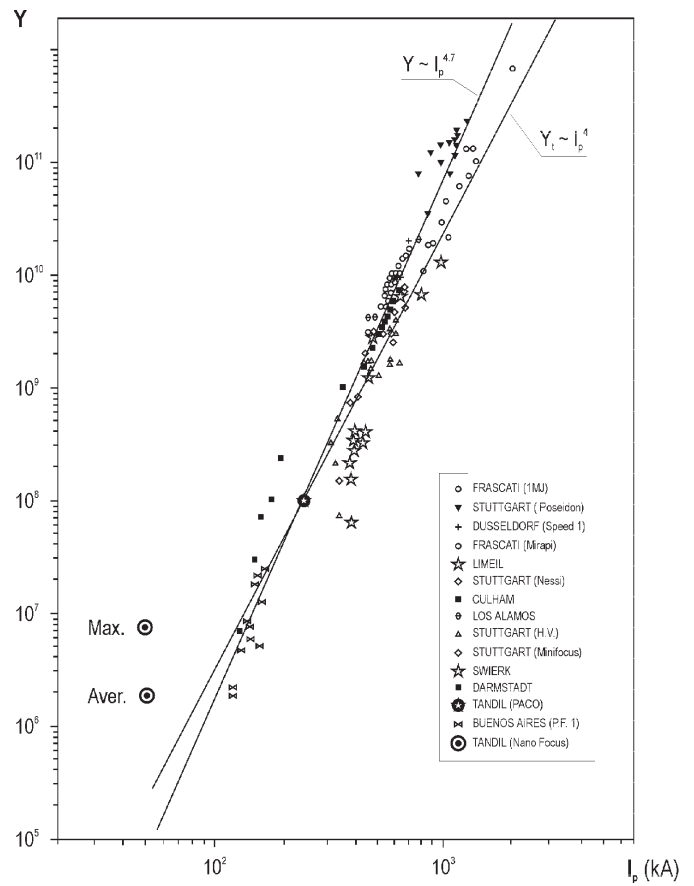


Fig. 3. Experimental points of neutron yield Y vs. pinch current I_p (in logarithmic scale) from more than a hundred plasma focus experiments, covering a wide range of energies, that fulfil the design criteria of reference [23]. The straight line Y_t corresponds to the thermonuclear model.

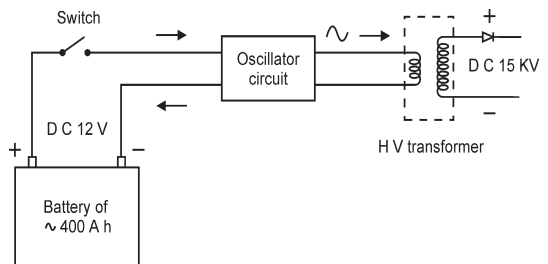


Fig. 4. Scheme of a portable power supply for the capacitor charge, based in a tractor battery.

of several experiments. In our case, we searched to get a neutron yield of about 10^6 neutrons per pulse from nuclear fusion in pure deuterium.

Based on the above mentioned ideas a Mather-type plasma focus is designed and constructed with the following general characteristics.

We chose a capacitor bank able to be charged by a battery. The power supply to be used in a transportable device, for example in rural areas, would be obtained on base of tractor battery in the way shown in Figure 4. Six condensers connected in parallel compose the bank. The

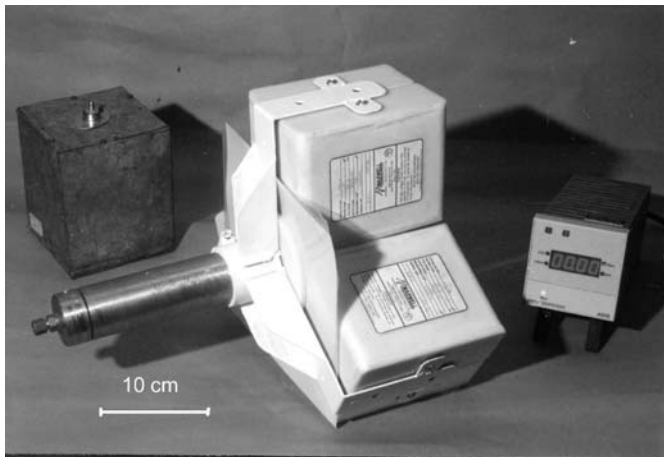


Fig. 5. General view of the Nanofocus with the capacitor bank in “star” disposition.

connection of the capacitors was very carefully studied in order to obtain a very low parasitic inductance. Firstly the capacitors were connected following a linear disposition: each one together the other, going with planar line to the spark gap and coaxial gun. The parameters in this case were the following: total capacitance $C = 1.1 \mu\text{F}$, parasitic inductance $L_0 = 74 \text{ nH}$, coaxial electrodes made in brass, anode (central electrode) diameter $\phi_i = 15 \text{ mm}$, anode free length $l = 22 \text{ mm}$, cathode inner diameter $\phi_0 = 42 \text{ mm}$, Pyrex insulator free length $l_i = 7 \text{ mm}$, just at the anode level (same diameter); a sharp edge is inserted at the back of the Pyrex tube. After we searched to make even more compact the generator and to diminish the parasitic inductance connecting the same capacitors ($1.1 \mu\text{F}$ of total capacity) in “star” disposition (Fig. 5). In order to achieve a good matching, we needed in this case to modify also other variables. The working parameters are now the following: anode diameter: 15 mm, Pyrex cylindrical insulator at the anode level; the parasitic inductance resulted 58.7 nH. We worked with three different anode free lengths: 10, 15 and 18 mm. The spark gap at atmospheric pressure is thought to give a very compact design.

3 Experimental systems for testing

A silver activation counter located side-on 0.5 m far from the Nanofocus is used to detect time-integrated neutron pulses. It consists in a 10-cm long Victoreen 1B85 Geiger-Müller counter wrapped in a 0.5 mm-silver foil and put into a 15 cm-sized paraffin block. The silver activation detector was calibrated with an Am-Be source that continuously emits 2.5 MeV neutrons. A scintillator-photomultiplier system located 1.5-m far from the device detects time-resolved neutron pulses. The plastic scintillator is a NE 102A that have a high response for 2.45 MeV neutrons originated in D-D fusion reactions. It is a solid cylinder whose dimensions are 18 cm of diameter and 5 cm of length. The plastic scintillator has a high efficiency for detecting also hard X-ray pulses (energy over

100 keV). We used a filter in order to attenuate hard X-rays pulses and then avoid the neutron pulses to be masked. A 3-mm thick lead sheet and a 1-mm thick copper sheet compose this X-ray filter. A 56 AVP Philips photomultiplier is optically coupled to the scintillator. The scintillator-photomultiplier detector is located in side-on position, 1.5 m far from the focus in order to distinguish the hard X-ray pulse from the neutron pulse because of the time-of-flight of 2.45 MeV neutrons. A Rogowski coil measures the total current flowing through the system. Both time-resolved signals: current derivative and scintillator-photomultiplier are registered simultaneously in a digital portable Tektronix TDS 3014 oscilloscope; both channels starts at the same time; the cables that transports both signals have the same length. The timing of the hard X-ray and neutron signals, include the transit time into the photomultiplier that is about 35 ns for the Philips 56 AVP at 1650 V used here. The time precision in the signals coming from scintillator-photomultiplier is about 5 ns (2 ns of rise-time in the scintillator and 3 in the photomultiplier). The Rogowski coil bandwidth is about 50 MHz; then it reproduces signals with rise-time higher than 10 ns. On the other hand, the oscilloscope time resolution is units of ns.

A scheme of the set-up used in our experiment can be seen in Figure 6a; in Figure 6b a picture containing a partial view of the experiment is shown.

4 Results and analysis

We will describe now the main results obtained. They involve an amount of approximately a thousand discharges. We found that, up to date, there are not very different results between both linear and “star” configurations. In this last, best results are obtained using an anode of 18-mm free length.

Series of discharges are made in pure deuterium at a pressure of around 2 mbar. The charging voltage of the capacitor bank was 16 kV. The maximum of the discharge current is 62 kA. Previous to the filling of the chamber with deuterium, it is evacuated at a pressure of 10^{-6} mbar. After the first discharge of each series, the pressure in the chamber results strongly elevated (about 0.1 mbar) because of the contamination of several materials, such as gases occluded in the walls or components of them. Then, we renewed the deuterium in each discharge. So, we computed only first discharges. We obtained about a ten-percent of successful events. The background measured by the silver activation counters (around 20 counts) would correspond to about 10^6 neutrons emitted in 4π sr. The so-named “successful events” are those that exceed at least by a factor 3 the background count. In Figure 7, a typical oscillogram obtained in a discharge of Nanofocus can be observed. The lower trace corresponds to a Rogowski’s current derivative signal. It can be observed (near the zero of the current derivative) a thin and very peaked dip, around the zero of the current derivative. This corresponds to a strong inductance variation because of the fast plasma

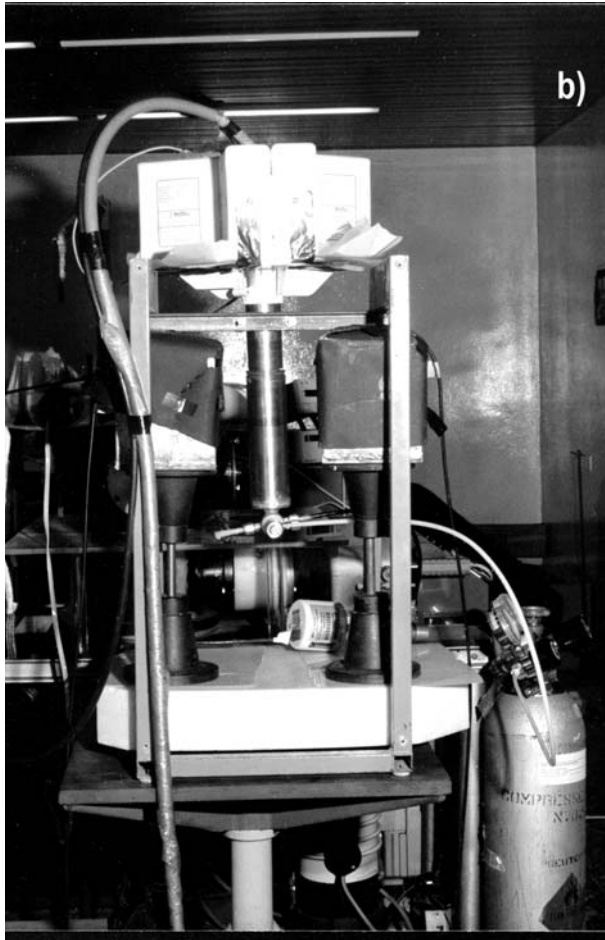
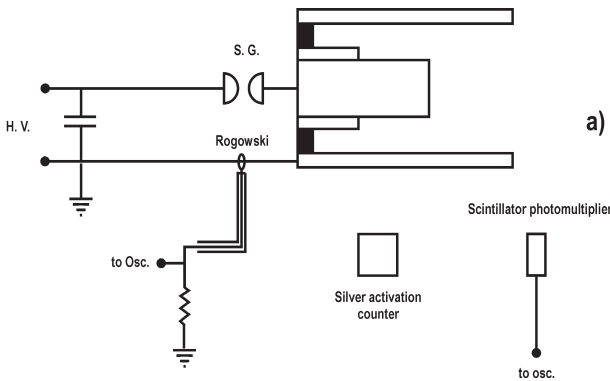


Fig. 6. (a) Schematic of the set-up; (b) partial view of the experimental arrangement.

column compression by pinch effect. As it can be seen this singular point on the sinusoidal curve occurs *circa* 400 ns from its beginning, lasting around 50 ns. During this stage the plasma column get a very high temperature (around 1 keV) and density (10^{20} cm^{-3}). As a consequence, thermonuclear fusion reactions are produced. Also, in the final part of this phase, $m = 0$ magneto-hydrodynamic instabilities mark several necking points in the column, where charge separation is produced. Then, the consequent strong electrical fields produce plasma electrons and ions acceleration and so very collimated and ener-

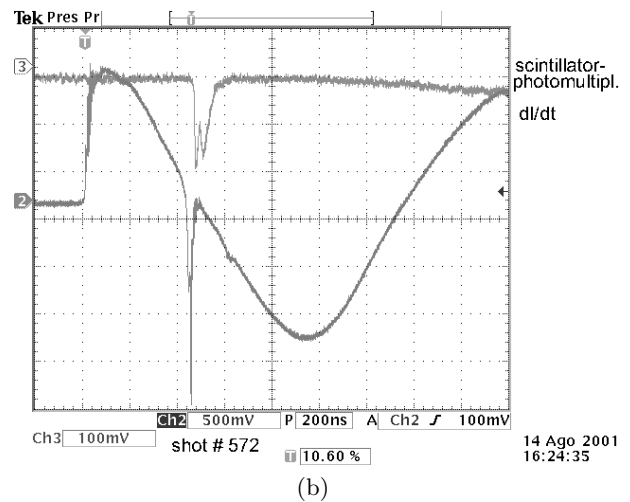
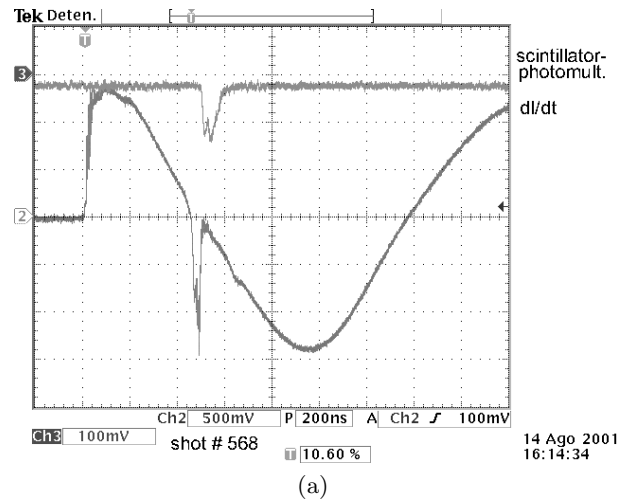


Fig. 7. Two typical oscillograms obtained in discharges of Nanofocus. The respective lower traces correspond to Rogowski's current derivative signals. The upper traces show the signals coming from the scintillator-photomultiplier detector.

getic electron beams strike the anode, producing a burst of X-rays. On the other hand, fast ion beams colliding with the bulk plasma and/or the residual deuterium, produces beam-target nuclear fusion reactions. The described process is observed in the upper trace of the oscilloscope (Fig. 7) where the signal coming from the scintillator-photomultiplier detector is shown. The first dip is the hard X-ray pulse. The X-ray filter described in the previous paragraph stops radiation of energy less than around two hundred keV [25]. As it can be observed in the oscillogram, the hard X-ray pulse begins when the variation of the current is maximum (in absolute value). *Circa* 80 ns later (that corresponds to the emitter-detector time-of-flight of 2.45 MeV neutrons) starts a pulse of fusion neutrons that lasts around 50 ns. This pulse is composed by the products of the two above-mentioned mechanisms of nuclear fusion: thermonuclear and beam-target. In a considerable amount (a 10%) of Nanofocus shots we obtained neutron yield not enough to exceed the background but certainly enough

to observe a pulse in the oscilloscope signal. In order to estimate the neutron yield of Nanofocus in these cases, a calibration is made in base to the discharges in which we have silver activation and scintillator-photomultiplier neutron data, previous numerical integration of the respective time-resolved neutron pulse. So we found that in these cases the 2.45 MeV neutron yield is of the order of 10^5 neutrons per pulse. Then, up to date, we got a 30% of the Nanofocus discharges yielding between 10^5 and 4×10^6 fusion neutrons per pulse.

5 Conclusions and comments

In this work we presented the Nanofocus device which was designed using criteria of design developed by our research group based in a MHD model. A non-minor problem of design that has been solved was the small size, compactness, transportability, easy charging voltage possibility; all this compatible with high efficiency in neutron production. The designed device was also constructed and tested. For the first time is here reported a relatively high fusion neutron yield (about 10^6 neutrons per pulse) and intense hard X-ray bursts in a device of so small stored energy (125 J). It must be noted that this machine has very high neutron efficiency in comparison with any other device (see the point corresponding to Nanofocus in Figure 3: neutron yield *vs.* pinch current).

Our experiment shows the feasibility of a very small device, transportable and suitable to be used far from fixed energy supplies, able for generating fast pulses of nuclear fusion neutrons and also hard X-ray pulses. A possible application very appreciate in agronomy is the measurement of soil humidity through the moderation of the Nanofocus neutron pulses in earth. This method will be a save-environment replacement of more traditional nuclear methods. It is also possible to detect dense materials in soil, constructions, etc, (neutronograph) and, using deuterium-tritium as filling gas, detect the presence of different materials (*i.e.* oil) through its nuclear activation by 14 MeV neutrons. As very brief hard X-ray pulses emitter could be used in a lot of applications where a very little and transportable source of such type of radiation is necessary.

This work is supported by a grant of the Agencia Nacional de Investigaciones Científicas y Tecnológicas of Argentina. We acknowledge the special collaboration of the technical team of our Laboratory: Mr. C. Santiago, Mr. N. Scali, Mr. H. Arislur, Mrs. E. Szyszkowski and Mr. S. Serrano.

References

1. J.W. Mather, in *Methods of Experim. Phys.*, edited by R. Lovberg, H. Griem (N. York Acad. Press 1971), Vol. 9B, p. 187
2. N.V. Filippov, *Sov. J. Plas. Phys.* **14**, 9 (1993)
3. J. Pouzo, H. Acuña, M. Milanese, R. Moroso, *Eur. Phys. J. D* **21**, 97 (2002)
4. M. Zakallah, K. Alamgir, M. Sharif, A. Waheed, G. Murtaza, *J. Fus. Energy* **19**, 143 (2000)
5. F. Castillo-Mejía, M. Milanese, R. Moroso, J. Pouzo, *J. Phys. D: Appl. Phys.* **30**, 1499 (1997)
6. Shyam, M. Srinivasam, *Appl. Phys.* **17**, 425 (1978)
7. Lee, T. Tou, S. Moo, M. Eissa, A. Golap, K. Kwek, S. Mulydrono, A. Smith, J. Suryadi, W. Usada, M. Zakallah, *Am. J. Phys.* **56**, 62 (1988)
8. K. Kwek, T. Tou, S. Lee, *IEEE Trans. Plas. Sci.* **18**, 826 (1990)
9. J. Pouzo, D. Cortázar, M. Milanese, R. Moroso, R. Píriz, *Small Plas. Phys. Experim.*, edited by S. Lee, P. Sakanaka (World Sci. Publ., London, 1988), pp. 80-100
10. H. Schmidt, "Generat., Phys. and Appl. of Super-dense Hot Z-Pinch Plasmas", Rep. on Activ., Univ. Stuttgart, Germany (Contr. SCI CT91-0728 (TSTS))
11. M. Sadowski, H. Schmidt, H. Herold, *Phys. Lett. A* **83**, 435 (1981)
12. A. Gentilini, Ch. Maisonnier, J.-P. Rager, *Comm. Plas. Phys.* **5**, 41 (1979)
13. M. Scholz, R. Miklaszewski, V. Gribkov, F. Mezzetti, *Nukleonika* **45**, 155 (2000)
14. F. Beg, I. Ross, A. Lorenz, J. Worley, J.A. Dangor, M. Haines, *J. Appl. Phys.* **88**, 3225 (2000)
15. F.N. Beg, K. Kruschelnik, C. Gower, S. Torn, A.E. Dangor, A. Howard, T. Sumner, A. Bewick, V. Lebedenko, J. Dawson, D. Davidge, M. Joshi, J.R. Gillespie, *Appl. Phys. Lett.* **80**, 3009 (2002)
16. R. Lebert, W. Neff, D. Rothweller, *J. X-Ray Sci. Technol.* **6**, 107 (1996); *Intern. Symp. Plas. (Jarnoltowek, Poland)* **1**, 121 (1997)
17. P. Lee, X. Feng, G.X. Zhang, M.H. Liu, S. Lee, *Plas. Sourc., Sci. Technol.* **6**, 343 (1997)
18. H. Conrads, *Proceed. of 3rd. Lat.-Am. Workshop in Plas. Phys.*, *Invit. Lect. Book*, Santiago, Chile, July 18-29, 1988, pp. 27-44 (1988)
19. F. Castillo-Mejía, M. Milanese, R. Moroso, J. Pouzo, M. Santiago, *IEEE Transac. Plas. Sci.* **29**, 921 (2001)
20. H. Acuña, M. Milanese, R. Moroso, J. Pouzo, *Book of Abstr. of the 85th Annual Meeting of "Asociación Física Argentina"*, Sept. 18-22, 2000, p. 95
21. M. Milanese, R. Moroso, J. Pouzo, *Book of Abstr. of the 86th Ann. Meet. of "Asoc. Física Argentina"*, Sept. 18-21, 2001, p. 69
22. J. Pouzo, M. Milanese, R. Moroso, *ICPP 2002*, Sydney, Australia, July 15-19, 2002, *AIP Conf. Proceed.* **669**, 277 (2003)
23. J. Vargas, F. Gratton., J. Gratton, H. Bruzzone, H. Kelly, *Proc. of the 6th. Int. Conf. on Plas. Phys. and Contr. Fusion Res.*, Berchtesgaden 1976, IAEA, Vienna (1976)
24. M. Milanese, J. Pouzo, *Small Plas. Phys. Experim.* (World Sci. Publ., London, 1988), pp. 66-79
25. J.H. Hubbell, S.M. Seltzer, *Ionizing Radiat. Div., Phys. Lab. Nat. Instit. of Standards and Techn. Gaithersburg, MD 20899*, "Tables of X-Ray Mass Attenuat. Coeffic. and Mass Energy-Absorpt. Coeffic. from 1 keV to 20 MeV for elements $Z = 1$ to 92 and 48 Addit. Substanc. of Dosimetric Interest", <http://physics.nist.gov/PhysRefData/XrayMassCoef>